Powerful harmonic charging in a quantum battery

Yu-Yu Zhang,[1,2,*] Tian-Ran Yang,[1] Libin Fu,[2,†] and Xiaoguang Wang[3,‡]
[1]*Department of Physics, Chongqing University, Chongqing 401330, China*
[2]*Graduate School, China Academy of Engineering Physics, Beijing 100193, China*
[3]*Zhejiang Institute of Modern Physics, Department of Physics, Zhejiang University, Hangzhou 310027, China*

(Received 5 December 2018; revised manuscript received 9 March 2019; published 8 May 2019)

We consider a harmonic charging field as an energy charger for the quantum battery, which consists of an ensemble of two-level atoms. The charging of noninteracting atoms is completely fulfilled, which exhibits a substantial improvement over previous static charging fields. Involving the repulsive interactions of atoms, the fully charging is achieved with shorter charged period over the noninteracting case, yielding an advantage for the charging. Excluding the charging field, a quantum phase transition is induced by the attractive atom-atom interactions, and the interacting atoms become degenerate in the ground state. We find that the degenerate states play a negative role in the charging due to the gapless energies. The atoms with strong attractive interactions can not be charged completely, which is accompanied by a drop of the maximum stored energy.

DOI: 10.1103/PhysRevE.99.052106

I. INTRODUCTION

Quantum information science develops very quickly in recent years. Various kinds of tasks using quantum information have been studied in detail such as quantum sensing, computations, and communications. Among these proposals, a quantum battery (QB) was proposed to use quantum effects such as quantum correlations to enhance the charging power and speed up the charging time in comparison with its classical counterpart [1–4]. The concept of a QB was originally proposed as a two-level system used to temporarily store energy transferred from an external field [5,6]. How to make efficient energy storage by exploiting nonclassical effects is a central and practical research subject.

Recent research efforts have been devoted to exploring contributions provided by quantum correlations for charging in collective QBs [6–11]. The Dicke QBs [7,8] describe collective QBs coupling to one common cavity, which serves as a global charger. The corresponding QB-charger coupling produces indirect interactions between QBs. Consequently, the advantage of quantum correlations of QBs mediated by the global charger has been explored in the charging power of the Dicke QBs. By contrast, there is another kind of QBs, in which the quantum correlations are induced by intrinsic interaction between QBs [10]. There is a physical phenomenon that shares many of the features with the quantum correlations in interacting systems—the quantum phase transition, which is induced by the change of a coupling parameter. It is interesting to study the properties of QBs in different phases related to quantum correlations, which should be in a close relation to the collective charging. For example, the connection between the phase transition induced by the QB-charger coupling and the optimal energy storage has recently been studied [7,8]. However, the effects of quantum correlations in the other kind of QBs with intrinsic interactions between batteries, especially a phase transition, have been overlooked. On the other hand, in all these studies QBs were investigated with a static charging field [5,6,8–10,12]. Although a harmonic driving as a charger has been studied numerically [4,7,11,13], an analytical solution for the harmonic charging remains elusive. It is challenging to solve a time-dependent Hamiltonian analytically to give an optimal driving frequency for the charging of the QB.

In this paper, we consider a QB system of N two-level atoms and a semiclassical harmonic field as a charger. The quantum correlations of the atoms rely on the interatomic infinite-range interactions. The charging of the QB with noninteracting atoms can be completely fulfilled, and the optimal driving frequency of the harmonic charger is obtained analytically. It exhibits a substantial improvement over the previous static charging field. Involving repulsive intrinsic interactions of atoms, the QB can be charged faster than that of noninteracting atoms, while the optimal charging period for the attractive interactions becomes longer as the coupling strength increases. For strong attractive interactions there occurs a quantum phase transition, which is accompanied by degenerate energies of the ground state. We find the maximal stored energy of the atoms in the degenerate phase drops from the fully charged value, which indicates that the gapless states play a negative role in the charging process.

The paper is outlined as follows. In Sec. II we study N two-level atoms charging independently by the harmonic field. The maximum stored energy and the optimal driving frequency are given analytically. In Sec. III we discuss contributions of the repulsive and attractive interatomic interactions in the process of energy storage. Finally, a brief summary is given in Sec. IV.

II. CHARGING FOR NONINTERACTING ATOMS

The QB consists of an ensemble of independent two-level atoms, which are collectively charged by a harmonic field

*yuyuzh@cqu.edu.cn
†lbfu@gscaep.ac.cn
‡xgwang1208@zju.edu.cn

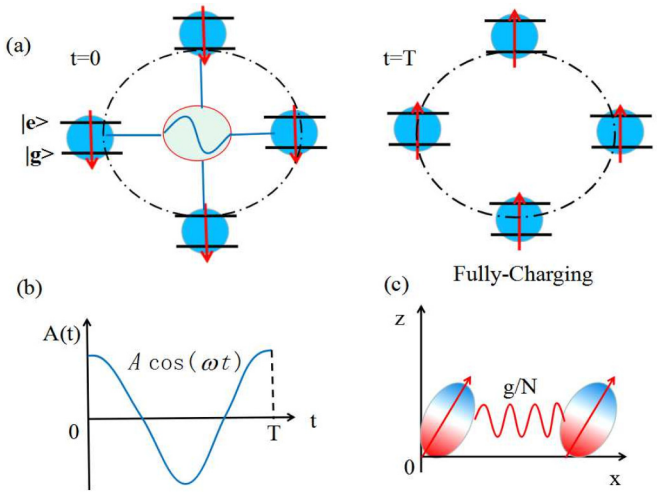

FIG. 1. (a) Charging protocol of N two-level atoms as the QB. At time $t = 0$ each atom is in the ground state $|g\rangle$. At the period T, the QB is fully charged, and the final state of atoms is $|e\rangle^{\otimes N}$. (b)The QB is charged with a harmonic driving field $A\cos(\omega t)$. During the charging time $0 < t < T$, the QB interacts with a harmonic driving field $A\cos(\omega t)$. Finally, the interaction is switched off at the end of charging period T. (c) The intrinsic infinite-range interactions between arbitrary two atoms include the repulsive ($g > 0$) and attractive ($g < 0$) coupling.

in Fig. 1(a). The Hamiltonian of N noninteracting atoms is given as

$$H_0 = \frac{\Delta}{2}\sum_{i=1}^{N}\sigma_i^z = \Delta S_z, \tag{1}$$

where the collective atom operators $S_\alpha = \sum_i \sigma_i^\alpha/2$ ($\alpha = x, y, z$), and Δ is the energy level splitting of the two-level atom. The basis set for representing the atoms system is the Dicke states $|S, m\rangle$ ($m = -S, -S+1, \ldots, S$), which are eigenstates of S^2 and S_z with the total pseudospin $S = N/2$. We set $\Delta = 1$ in the following.

We employ a harmonic field as a charger to transfer energy to the battery as much as possible. All two-level atoms are driven by the harmonic charging field as

$$H_1 = \frac{A}{2}\cos(\omega t)\sum_{i=1}^{N}\sigma_i^x = A\cos(\omega t)S_x, \tag{2}$$

where A and ω are the driving amplitude and the modulated frequency. For a comparison, the driving Hamiltonian with a static charging field is $H_{1,s} = AS_x$. It is noted that the coupling between QB and the harmonic charger is the conchoidal function of time instead of a constant in the static charger. Figure 1(b) shows the charging procedure is designed to turn on the interaction between N atoms and the harmonic field during the charging interval $0 < t < T$. Then the interaction is turned off at time T, and the QB is isolated from the external field and keeps its energy. The charging period is associated with the alternative driving frequency as $T = 2\pi/\omega$. During the charging step, the total Hamiltonian for N two-level atoms interacting with the harmonic field is $H = H_0 + H_1$, which is viewed as the collective Hamiltonian.

To study the advantage for the charging with the harmonic charging field, we focus on maximizing the stored energy in the QB and minimizing the charging time. Initially, N two-level atoms are prepared in the lowest-energy state as $|\varphi_N(0)\rangle = |N/2, -N/2\rangle$, for which each atom is in the ground state $|g\rangle$. The wave function evaluates according to the Schrödinger equation $i\partial|\varphi_N(t)\rangle/\partial t = H|\varphi_N(t)\rangle$. At the end of charging period T, the stored energy that moves from the harmonic field to the QB can be expressed in terms of the mean local energy of the QB [7,10]:

$$E_N(T) = \langle\varphi_N(T)|H_0|\varphi_N(T)\rangle - \langle\varphi_N(0)|H_0|\varphi_N(0)\rangle. \tag{3}$$

A battery is a physical system that stored energy in atoms, which is transferred from the charging field. We investigate the maximum stored energy $E_{N,\max}$ during the charging process. The advantage of the harmonic field lies in the modulated frequency ω, which can be tuned to produce maximum stored energy $E_{N,\max}$ at an optimal charging period $T_{\max} = 2\pi/\omega_{\max}$. As the QB is charged completely, each of the two-level atoms is in the upper state, and the scaled stored energy $E_{\max}(T)/N\Delta$ is expected to be the fully charging value 1. The corresponding final state at the end of the charging is

$$|\varphi_N(T_{\max})\rangle = |e\rangle^{\otimes N}, \tag{4}$$

which is called the fully charging state in Fig. 1(a).

Inspired by the approximated analytical solution for the driven semiclassical Rabi model for a driving two-level system [14], we extend the approach to solve the dynamics of N two-level atoms analytically. Using a unitary transformation $U = \exp[i\frac{A}{\omega\sqrt{N}}\xi\sin(\omega t)S_x]$ with the undetermined parameter $\xi \in [0, 1]$, one obtains $H' = UHU^\dagger - iU\frac{d}{dt}U^\dagger$ as

$$H' = \Delta\left\{\cos\left[\frac{A}{\omega\sqrt{N}}\xi\sin(\omega t)\right]S_z + \sin\left[\frac{A}{\omega\sqrt{N}}\xi\sin(\omega t)\right]S_y\right\} + A\left(1 - \frac{\xi}{\sqrt{N}}\right)\cos(\omega t)S_x. \tag{5}$$

We expand the operator identities $\cos[\frac{A}{\omega\sqrt{N}}\xi\sin(\omega t)] = J_0(\frac{A}{\omega\sqrt{N}}\xi) + 2\sum_{n=1}^{\infty}J_{2n}(\frac{A}{\omega\sqrt{N}}\xi)\cos(2n\omega t)$ and $\sin[\frac{A}{\omega\sqrt{N}}\xi\sin(\omega t)] = 2\sum_{n=0}^{\infty}J_{2n+1}(\frac{A}{\omega\sqrt{N}}\xi)\sin[(2n+1)\omega t]$, where $J_n(\frac{A}{\omega\sqrt{N}}\xi)$ denotes the Bessel function of integer order n. Then we reasonably neglect all higher-order harmonic terms ($n \geqslant 2$) with the higher-order Bessel functions $J_n(\frac{A}{\omega\sqrt{N}}\xi)$. The Hamiltonian is approximated as

$$H' = \Delta J_0\left(\frac{A}{\omega\sqrt{N}}\xi\right)S_z + A\left(1 - \frac{\xi}{\sqrt{N}}\right)\cos(\omega t)S_x + 2\Delta J_1\left(\frac{A}{\omega\sqrt{N}}\xi\right)\sin(\omega t)S_y. \tag{6}$$

The Hamiltonian includes the counter-rotating (CR) terms $e^{i\omega t}S_+ + e^{-i\omega t}S_-$ and the rotating-wave terms $e^{i\omega t}S_- + e^{-i\omega t}S_+$. Since the CR terms describe fast oscillation and virtual atom-field interacting processes, it is reasonable to make these terms vanish. We can choose the parameter ξ to

tune the coefficient of the CR terms to be zero, giving

$$A\left(1-\frac{\xi}{\sqrt{N}}\right)-2\Delta J_1\left(\frac{A}{\omega\sqrt{N}}\xi\right)=0. \tag{7}$$

Then ξ is determined as $\bar{\xi}$. Consequently the transformed Hamiltonian becomes

$$H''=\Delta J_0\left(\frac{A}{\omega\sqrt{N}}\bar{\xi}\right)S_z+\tilde{A}(e^{i\omega t}S_-+e^{-i\omega t}S_+), \tag{8}$$

where $\Delta J_0(\frac{A}{\omega\sqrt{N}}\bar{\xi})$ is the renormalized atomic transition frequency, and $\tilde{A}=\frac{A}{2}(1-\frac{\bar{\xi}}{\sqrt{N}})$ is the effective coupling strength between the QB and the charging field.

Using a unitary transformation $S=\exp(-i\omega t S_z)$, the time-independent Hamiltonian $\tilde{H}=SH''S^\dagger-iSdS^\dagger/dt$ is given by

$$\tilde{H}=\tilde{\Delta}S_z+2\tilde{A}S_x, \tag{9}$$

where the effective detuning is

$$\tilde{\Delta}=\Delta J_0\left(\frac{A}{\omega\sqrt{N}}\bar{\xi}\right)-\omega. \tag{10}$$

In the rotating frame, $\tilde{H}$ can be solved independent on the time. By contrast to a static charging field, the advantage of the harmonic charger lies in the renormalized detuning $\tilde{\Delta}$ and the effective QB-charger coupling strength $\tilde{A}$ of the effective Hamiltonian $\tilde{H}$, which can be tuned by the driving frequency ω.

The charging of N noninteracting atoms is equivalent to parallel charging for independent atoms, and the scaled stored energy $E_N/(N)$ equals E_1 of the single-atom battery. So we focus on the energy storage in the single atom. For $N=1$, the effective Hamiltonian $\tilde{H}$ (9) with $S=1/2$ can be solved analytically. The eigenvalues are given as $\varepsilon_\pm=\pm\Omega_R/2$, where Ω_R is the effective Rabi frequency

$$\Omega_R=\sqrt{\tilde{\Delta}^2+4\tilde{A}^2}. \tag{11}$$

The corresponding eigenstates are dressed states $\sin\theta|\mp z\rangle\pm\cos\theta|\pm z\rangle$ with $\tan(2\theta)=2\tilde{A}/\tilde{\Delta}$, where $|\pm z\rangle$ are the eigenstates of S_z.

At the end of the charging protocol, the final state of the one-atom battery is given explicitly by the eigenstates and eigenvalues as

$$|\varphi_1(T)\rangle=-i\frac{2\tilde{A}}{\Omega_R}\sin(\varepsilon_+T)|e\rangle+\left[\cos(\varepsilon_+T)+i\frac{\tilde{\Delta}}{\Omega_R}\sin(\varepsilon_+T)\right]|g\rangle. \tag{12}$$

The corresponding stored energy in the single-atom battery is

$$E_1(T)/\Delta=\frac{2\tilde{A}^2}{\Omega_R^2}[1-\cos(\Omega_RT)]. \tag{13}$$

The analytical stored energy $E_1(T)/\Delta$ is consistent with numerical results in a wide range of the charging period T in Fig. 2.

At the optimal period $T_{\max}=n\pi/\Omega_R$(for odd integer $n=1,3,\ldots$), the maximal value of the stored energy in Eq. (13) is given as

$$E_{1,\max}/\Delta=\frac{4\tilde{A}^2}{\tilde{\Delta}^2+4\tilde{A}^2}. \tag{14}$$

The corresponding optimal driving frequency $\omega_{\max}$ is determined as $2\pi/T_{\max}=2\Omega_R/n$. Figure 2 shows that the stored energy $E_1(T)/\Delta$ has local maximal values at a few peaks, which depends on the optimal charging period $T_{\max}$ with the odd integer n. It is obvious that $E_{1,\max}/\Delta$ in Eq. (14) ranges from 0 to 1 dependent on the effective transition frequency of atoms $\tilde{\Delta}$ in Eq. (10), which is a function of the driving frequency ω. In particular, one can achieve the fully charging value $E_{1,\max}/\Delta=1$ by modulating ω to satisfy $\tilde{\Delta}=0$. It leads to the fully charging condition

$$\omega_{\max}=\Delta J_0\left(\frac{A}{\omega}\bar{\xi}\right) \tag{15}$$

with $\bar{\xi}$ determined in Eq. (7). The final state $|\varphi_1(T)\rangle$ in Eq. (12) evaluates to be $|e\rangle$, which demonstrates that each atom is completely charged.

Figure 3 displays the maximum stored energy $E_{1,\max}/\Delta$ for different driving amplitude A. The contour projection of $E_{1,\max}/\Delta$ presents the optimal frequency $\omega_{\max}$. As A increases to 1, $E_{1,\max}/\Delta$ increases to 1 and then decreases. The maximum stored energy has a jump around $A=1.2$. It ascribes to the discontinuous jump of the optimal frequency $\omega_{\max}$ with the odd integer n changing from 1 to 3.

For a comparison, the Hamiltonian of the QB coupled with the static charging field is $H_s=\Delta S_z+AS_x$. Similarly, at the end of charging time T the energy stored in the battery is

$$E_s(T)/\Delta=\frac{1}{2}\frac{A^2}{\Delta^2+A^2}[1-\cos(\sqrt{\Delta^2+A^2}T)]. \tag{16}$$

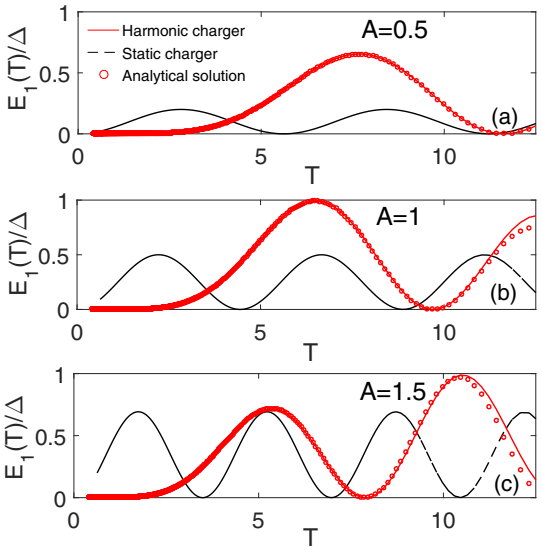

FIG. 2. Stored energy $E_1(T)/\Delta$ in the single-atom battery as a function of charging period T for driving amplitude $A=0.5$ (a), $A=1$ (b), and $A=1.5$ (c). The QB couples to the harmonic charger $A\cos(\omega t)$ (red sold line) and the static charger A (black dashed line), respectively. The analytical results of $E_1(T)/\Delta$ in Eq. (13) for the harmonic charging filed are shown in the red circle.

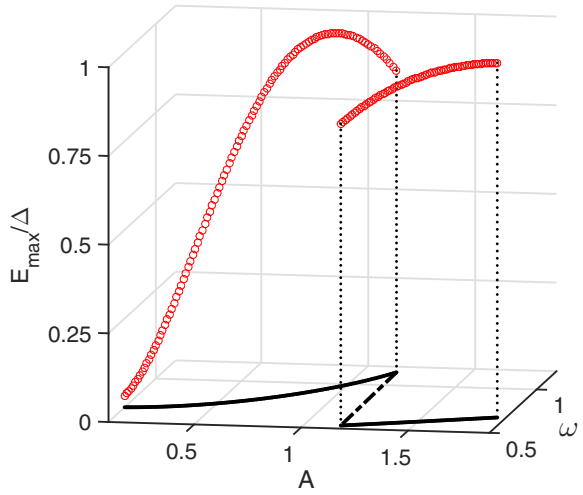

FIG. 3. Maximum stored energy $E_{\max}/\Delta$ (red circles) in the single-atom battery as a function of the driving frequency ω and the amplitude A of the harmonic charger $A\cos(\omega t)$. The contour projection displays the optimal frequency $\omega_{\max}$ (solid black line) dependent on A.

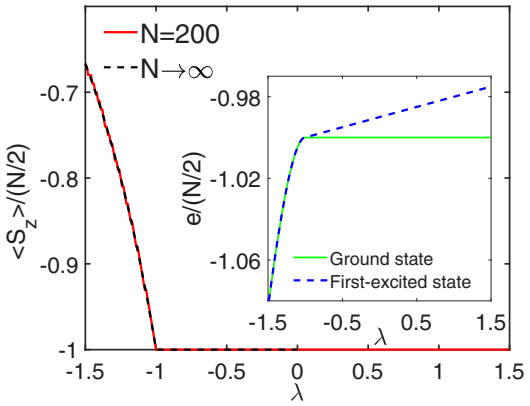

FIG. 4. $\langle S_z\rangle/(N/2)$ as a function of the repulsive and attractive coupling strength λ for $N = 200$ atoms. The analytical results of $\langle S_z\rangle/(N/2)$ for the infinite atoms $N \to \infty$ display the quantum phase transition at $\lambda_c = -1$ in the attractive interactions case (black dashed line). The inset shows the scaled energy $e/(N/2)$ for the ground state(green solid line) and the first-excited state energy (blue dashed line) dependent on λ.

Obviously, the maximum stored energy is given by $E_{s,\max}/\Delta = A^2/(\Delta^2 + A^2)$. It is impossible to achieve the fully charging value $E_{s,\max} = 1$. It means that the charging of the QB with a static charging field is not completely fulfilled. The maximum stored energy with the harmonic charging field is larger than that with the static charging field in Fig. 2, exhibiting the powerful harmonic charging.

III. COLLECTIVE CHARGING WITH INTERATOMIC CORRELATIONS

With the consideration of additional interatomic interactions, a quite natural question follows as to the effects on the charging battery. Quantum correlations in multipartite systems are connected to energy storage [1,5,6,9]. It is interesting to study the positive and negative effects of the quantum correlations induced by intrinsic interactions of two-level atoms in the charging of the QB.

For N identical two-level atoms, long-range forces between all atoms can be mediated by the electric field. Such long-range interactions can be engineered and controlled using atoms trapped in a photonic crystal waveguide [15] and Bose-Einstein condensed atoms [16], which highlight the practical relevance for the interacting Hamiltonian considered here. Each two-level atom is polarized in Fig. 1(c), which can be described as an electric dipole operator $\hat{d} = d\sigma_+ + d^*\sigma_-$ with the dipole momentum d and d^*. Involving the infinite-range dipole-dipole interactions, the Hamiltonian of N interacting atoms can be described by [17,18]

$$H_0^I = \frac{\Delta}{2}\sum_{i=1}^{N}\sigma_i^z + \frac{g}{2N}\sum_{i\neq j}^{N}\left(\sigma_i^x\sigma_j^x + \sigma_i^y\sigma_j^y\right) = \Delta S_z + \frac{g}{N}\left(S^2 - S_z^2 - \frac{N}{2}\right), \quad (17)$$

where g is the atom-atom coupling strength including the repulsive ($g > 0$) and attractive ($g < 0$) interactions. We define the scaled coupling strength $\lambda = g/\Delta$.

The interacting Hamiltonian H_0^I describes long-range interactions in two-level systems such as the Lipkin-Meshkov-Glick (LMG) model [19,20]. The ground state of H_0^I in Eq. (17) lies in the subspace spanned by the Dicke states $\{|N/2, M\rangle, M = -N/2, \ldots, N/2\}$ with the total spin $S = N/2$, which is the eigenstate of S_z with the eigenvalue M. The Hamiltonian reduces into two spaces dependent on even or odd values of $(N/2 - M)$, and it is denoted as parity. The interacting atoms with attractive interactions ($g < 0$) undergo a quantum phase transition due to the competition between the first noninteracting term and the second interacting terms of H_0^I. For a weak attractive coupling strength, the even and odd levels are obviously separated. The ground state is fully polarized in the Z direction and is given as $|N/2, -N/2\rangle$. When λ exceeds the critical attractive coupling strength, the even and odd levels become degenerate in the thermodynamical limit. The inset of Fig. 4 displays that energy levels $e/(N/2)$ of $N = 200$ atoms in the ground state and the first-excited state are almost degenerate for $\lambda < -1$. However, for arbitrary repulsive coupling strength ($g > 0$), the ground state remains $|N/2, -N/2\rangle$ with the lowest energy $-\Delta N/2$, and the energy levels are nondegenerate.

To explore the phase transition in the attractive interactions, we now use the Hosltein-Primakoff transformation to study the infinite atoms in terms of auxiliary bosonic operators $b^\dagger$ and b: $S_z = b^\dagger b - N/2$ and $S_+ = b^\dagger\sqrt{N}$. Above the critical coupling value λ_c, the bosonic field is expected to shift with a value β as $b^\dagger \to b^\dagger + \beta$. We then obtain the approximated Hamiltonian

$$\tilde{H}_0^I = \Delta\left[(b^\dagger+\beta)(b+\beta) - \frac{N}{2}\right] + \frac{g}{N}\left\{\frac{N^2}{4} - \left[(b^\dagger+\beta)(b+\beta) - \frac{N}{2}\right]^2\right\}. \quad (18)$$

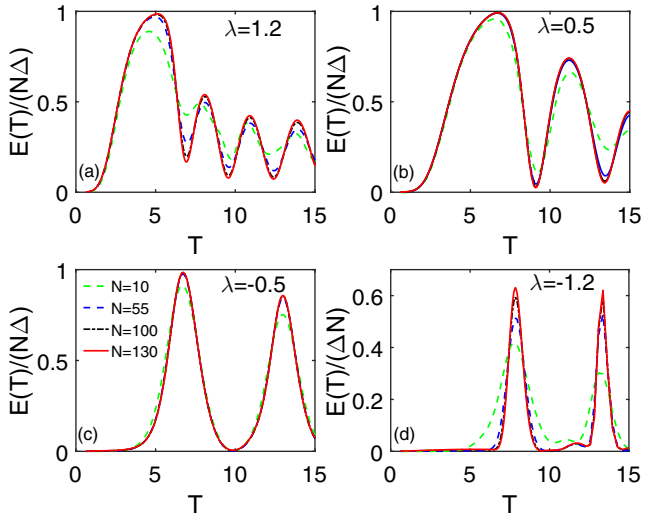

FIG. 5. Stored energy $E_N(T)$ (in unit of $N\Delta$) as a function of charging period T for different N with interatomic coupling strength $\lambda = 1.2$ (a), $\lambda = 0.5$ (b), $\lambda = -0.5$ (c), and $\lambda = -1.2$ (d). The driving amplitude is $A = 1$.

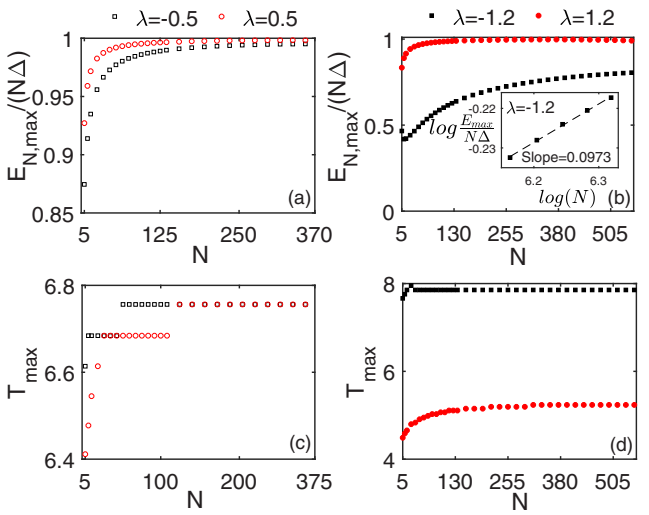

FIG. 6. Maximum stored energy in the battery $E_{N,\max}/(N\Delta)$ and the optimal charging period $T_{\max}$ as a function of atoms number N for interatomic coupling strength $\lambda = \pm 0.5$ (open circle) (a), (c) and $\lambda = \pm 1.2$ (solid circle) (b), (d), respectively. For $\lambda = -1.2$, the inset shows $E_{\max}/(N\Delta)$ versus N on a log-log scale, showing the slope of the scaling line 0.0973 (b).

To make the linear terms $(b^\dagger + b)$ vanish, one obtain

$$\beta^2 = N(g + \Delta)/(2g). \tag{19}$$

Obviously, the critical value is given by $\lambda_c = g_c/\Delta = -1$. Above the critical value, the expected value of atom polarization in the ground state is given by $\langle S_z\rangle = \beta^2 - N/2$. Figure 4 shows the behavior of the polarized value per atom $\langle S_z\rangle/(N/2)$ for infinite atoms $N \to \infty$, exhibiting a quantum phase transition at $\lambda_c = -1$.

It is interesting to study whether the attractive and repulsive interactions, especially the phase transition, can enhance the charging of the QB. The stored energy in the N interacting atoms can be expressed as

$$E_N(T) = \langle\varphi_N(T)|H_0^I|\varphi_N(T)\rangle - \langle\varphi_N(0)|H_0^I|\varphi_N(0)\rangle, \tag{20}$$

where the state evaluates according to $i\partial|\varphi_N(T)\rangle/\partial t = (H_0^I + H_1)|\varphi_N(T)\rangle$ with the charging harmonic field H_1 in Eq. (2). Due to the intrinsic many-body interactions, the energy stored in the interacting atoms is in general a complicated function of the charging period T.

We numerically calculate the stored energy $E_N(T)$ dependent on the coupling strength λ for the driving amplitude $A = 1$. The dependence of the rescaled stored energy $E_N/(N\Delta)$ on the charging period T is shown in Fig. 5. We observe the maximum stored energy $E_{N,\max}(T) \equiv \max_T E_N(T)$ locates at the first peak, where the optimal charging period $T_{\max}$ is determined. The corresponding optimal driving frequency is given by $\omega_{\max} = 2\pi/T_{\max}$.

As the system size N increases to 600, $E_{N,\max}/(N\Delta)$ converges to be 1 for the repulsive coupling strength $\lambda = 0.5$ and 1.2 in Figs. 6(a) and 6(b). For the attractive interacting atoms with $\lambda = -1.2$, $E_{\max}/(N\Delta)$ also converges with a lower value in Fig. 6(b), for which the slope of the scaling line approaches zero. It demonstrates that the scaling law of the maximum stored energy for the repulsive and attractive interacting atoms is

$$E_{N,\max} \propto N, \tag{21}$$

which is the same as the results of the Dicke quantum battery [7]. On the other hand, the optimal charging period $T_{\max}$ converges to the same value for weak attractive and repulsive coupling strength $\lambda = \pm 0.5$ in Fig. 6(c). However, as the attractive interactions become strong with $\lambda = -1.2$, $T_{\max}$ becomes longer than that for the repulsive coupling strength $\lambda = 1.2$ in Fig. 6(d).

Furthermore, the maximum stored energy $E_{\max}/(N\Delta)$ and the optimal charging period $T_{\max}$ depending on the coupling strength are calculated in Fig. 7. It is observed that $E_{\max}/(N\Delta)$ approaches the fully charged value 1 in a wide range of the repulsive coupling strengths. As the attractive coupling strength gets close to the critical value $\lambda_c = -1$, the maximum energy stored gets worse and drops sharply from 1 in Fig. 7(a). Meanwhile, $T_{\max}$ for the attractive coupling strength is longer

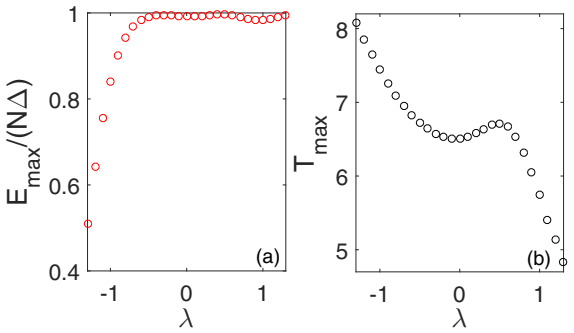

FIG. 7. (a) Maximum stored energy $E_{\max}$ (in unit of $N\Delta$) and (b) the optimal charging period $T_{\max}$ dependent on the interatomic coupling strength λ for $N = 140$ atoms.

over the noninteracting case $\lambda = 0$. By contrast, the charging for strong repulsive interacting atoms with $\lambda > 0$ is faster in Fig. 7(b). It reveals that the strong repulsive interactions of atoms play a positive role in the charging, which can speed up the charging of the interacting atoms.

Since the phase transition of the attractive interacting atoms is induced by the first noninteracting Δ-term and the second coupling g-term of the Hamiltonian H_0^I in Eq. (17). The low energy of the first noninteracting term is responsible for charging between the states $|g\rangle$ and $|e\rangle$ for each atom. As the attractive coupling strength increases, the evolution is dominated by the high-energy part of the second g-term. The high-energy eigenstates can influence the charging states of the many-body battery, which play a negative role in the charging. However, the direct correlations between the phase transition and the charging remain unclear due to the complicated evolution in the interacting atoms.

IV. CONCLUSION

In this work, we introduce the harmonic driving field as the energy charger for the quantum battery, which consists of N two-level atoms. By contrast to previous studies with a static charging field, the quantum battery of noninteracting atoms can be fully charged by choosing an optimal driving frequency. After the charging process, each of the two-level atoms is finally in the upper state. Involving the intrinsic interactions between atoms, two important effects are clearly seen: (1) the repulsive interactions in large N atoms can enhance the fully charging with shorter charging period, yielding an advantage in charging over the noninteracting atoms; (2) for the attractive interactions case, the quantum phase transition with degenerate energies plays a negative role in the energy storage in this quantum battery. The maximum stored energy of the QB in the degenerate phase drops sharply from the fully charging value with longer charging period.

In terms of outlook, the two-level quantum battery we discuss here could be a physically realizable scheme. Recently, experimental efforts have been devoted to quantum simulations of an array of two-level systems, such as with a solid-state platform [7,21], trapped ions [22], and cold atoms [16], which could be considered as quantum battery. When charging resources such as Raman laser beams with modulated frequency are driven onto such two-level systems, the charging of the quantum battery with a harmonic field could be implemented realistically. The kind of quantum battery facilitates the exploitation of the contributions of the quantum correlations of many-body systems for a charging process, especially the effects of quantum phase transitions.

ACKNOWLEDGMENTS

This work was supported by National Natural Science Foundation of China (Grant No. 11847301) and by the Fundamental Research Funds for the Central Universities of China (Grants No. 2019CDXYWL0029 and No. 2019CDJDWL0005). F.L.B. acknowledges the support from the National Natural Science Foundation of China (Grants No. 11725417, No. 11575027, and No. 11475146) and NSAF (Grant No. U1730449). X.G.W. acknowledges support from the National Natural Science Foundation of China (Grant No. 11875231) and the National Key Research and Development Program of China (Contracts No. 2017YFA0304202 and No. 2017YFA0205700).

[1] K. V. Hovhannisyan, M. Perarnau-Llobet, M. Huber, and A. Acín, Phys. Rev. Lett. **111**, 240401 (2013).
[2] N. Friis, M. Huber, and M. Perarnau-Llobet, Phys. Rev. E **93**, 042135 (2016).
[3] N. Friis and M. Huber, Quantum **2**, 61 (2018).
[4] D. Farina, G. M. Andolina, A. Mari, M. Polini, and V. Giovannetti, Phys. Rev. B **99**, 035421 (2019).
[5] R. Alicki and M. Fannes, Phys. Rev. E **87**, 042123 (2013).
[6] F. Binder, S. Vinjanampathy, K. Modi, and J. Goold, New. J. Phys. **17**, 075015 (2015).
[7] D. Ferraro, M. Campisi, G. M. Andolina, V. Pellegrini, and M. Polini, Phys. Rev. Lett. **120**, 117702 (2018).
[8] L. Fusco, M. Paternostro, and G. D. Chiara, Phys. Rev. E **94**, 052122 (2016).
[9] F. Campaioli, F. A. Pollock, F. C. Binder, L. Celeri, J. Goold, S. Vinjanampathy, and K. Modi, Phys. Rev. Lett. **118**, 150601 (2017).
[10] T. P. Le, J. Levinsen, K. Modi, M. M. Parish, and F. A. Pollock, Phys. Rev. A **97**, 022106 (2018).
[11] G. M. Andolina, D. Farina, A. Mari, V. Pellegrini, V. Giovannetti, and M. Polini, Phys. Rev. B **98**, 205423 (2018).
[12] F. Campaioli, F. A. Pollock, and S. Vinjanampathy, arXiv:1805.05507v1.
[13] G. M. Andolina, M. Keck, A. Mari, M. Campisi, V. Giovannetti, and M. Polini, Phys. Rev. Lett. **122**, 047702 (2019).
[14] Y. Y. Yan, Z. Lu, and H. Zheng, Phys. Rev. A **91**, 053834 (2015).
[15] C. L. Hung, A. González-Tudela, J. I. Cirac, and H. J. Kimble, Proc. Natl. Acad. Sci. USA, **113**, E4946 (2016)
[16] K. Baumann, C. Guerlin, F. Brennecke, and T. Esslinger, Nature (London) **464**, 1301 (2010).
[17] Q. H. Chen, T. Liu, Y. Y. Zhang, and K. L. Wang, Phys. Rev. A **82**, 053841 (2010).
[18] G. Chen, X. G. Wang, J. Q. Liang, and Z. D. Wang, Phys. Rev. A **78**, 023634 (2008).
[19] N. Meshkov, A. J. Glick, and H. J. Lipkin, Nucl. Phys. **62**, 199 (1965); H. J. Lipkin, N. Meshkov, and A. J. Glick, *ibid.* **62**, 188 (1965)
[20] H. T. Quan, Z. D. Wang, and C. P. Sun, Phys. Rev. A **76**, 012104 (2007).
[21] P. Forn-DÍaz, J. J. GarcÍa-Ripoll, B. Peropadre, J.-L. Orgiazzi, M. A. Yurtalan, R. Belyansky, C. M. Wilson, and A. Lupascu, Nat. Phys. **13**, 39 (2016).
[22] D. Lv, S. An, Z. Liu, J. N. Zhang, J. S. Pedernales, L. Lamata, E. Solano, and K. Kim, Phys. Rev. X **8**, 021027 (2018).